1	Synthesis, Crystal Structures and Catalytic Property of Dioxomolybdenum(VI)			
2	and Nickel(II) Complexes Derived from bis-Schiff bases			
3				
4	Ling-Wei Xue*, Qin-Long Peng, Pan-Pan Wang, Hui-Jie Zhang			
5				
6	College of Chemistry and Chemical Engineering, Pingdingshan University,			
7	Pingdingshan Henan 467000, P.R. China			
8	*E-mail: pdsuchemistry@163.com			
9				
10	Abstract			
11	A new mononuclear dioxomolybdenum(VI) complex, [MoO ₂ L ¹], and a new linear			
12	trinuclear nickel(II) complex, $[Ni\{NiL^2(\mu_1-\eta^1:\eta^0-OAc)(\mu_2-\eta^1:\eta^1-OAc)\}_2]\cdot H_2O$, where			
13	L^1 is the dianionic form of N,N' -bis(5-fluorosalicylidene)-1,3-propanediamine (H_2L^1),			
14	L^2 is the dianionic form of			
15	N,N'-bis(5-fluoro-2-hydroxybenzylidene)-2-hydroxy-1,3-propanediamine (H ₂ L ²),			
16	have been synthesized and characterized by elemental analysis, FT-IR spectra, and			
17	single crystal X-ray determination. The Mo atom in the molybdenum complex is			
18	coordinated by four donor atoms of the Schiff base ligand, and two oxo groups,			
19	forming an octahedral coordination. In the nickel complex, there are three bridges			
20	across the Ni-Ni atom pairs, involving two phenolate O atoms of a Schiff base ligand,			
21	and an O-C-O moiety of a μ_2 - η^1 : η^1 -OAc group. The central Ni atom is located on an			
22	inversion center and has octahedral coordination involving four bridging O atoms			
23	from two Schiff base ligands in the equatorial plane and two O atoms from two			
24	μ_2 - η^1 : η^1 -OAc ligands in the axial positions. The coordination around the terminal Ni			
25	atoms is also octahedral, with two imino N and two phenolate O atoms from a Schiff			
26	base ligand defining the equatorial plane, and with two O atoms respectively from a			
27	$\mu_1 - \eta^1 : \eta^0$ -OAc and a $\mu_2 - \eta^1 : \eta^1$ -OAc ligands occupying the axial positions. The			
28	molybdenum complex has excellent catalytic property for sulfoxidation reactions.			
29				
30	Keywords: dioxomolybdenum complex, nickel complex, Schiff base, Crystal			
31	structure, Sulfoxidation			
32				
33	1. Introduction			
34	Molybdenum and nickel complexes with multi-dentate ligands have received			

remarkable attention in recent years for their catalytic properties¹ and molecular structures.² Salicylaldehyde and its derivatives have been widely used as ligands for the preparation of metal complexes with various applications.³ A large number of molybdenum and nickel complexes with Schiff bases have been reported.⁴ Some of the complexes have shown oxygen atom transfer properties as they were found to oxidize thiols, hydrazine, polyketones, and tertiary phosphines.⁵ Recently, we have reported some molybdenum and manganese complexes derived from hydrazone type ligands, and show interesting catalytic properties. We report in this paper the syntheses, crystal structures and catalytic property of a new dioxomolybdenum(VI) complex, [MoO₂L¹], and a new linear trinuclear nickel(II) $[Ni\{NiL^2(\mu_1-\eta^1:\eta^0-OAc)(\mu_2-\eta^1:\eta^1-OAc)\}_2]\cdot H_2O$, where L^1 is the dianionic form of N.N'-bis(5-fluorosalicylidene)-1,3-propanediamine (H_2L^1), L^2 is the dianionic form of *N*,*N*'-bis(5-fluoro-2-hydroxybenzylidene)-2-hydroxy-1,3-propanediamine (H_2L^2) : Scheme 1).

49 E ^ >

Scheme 1. The Schiff base ligands H₂L¹ and H₂L²

5152

53

54

55

56

57

58

59

60

61

62

63

64

65

50

35

36

37

38

39

40

41

42

43

44

45

46

47

48

2. Experimental

2.1. Materials and methods

5-Fluorosalicylaldehyde, propane-1,3-diamine and 2-hydroxyl-1,3-propanediamine were purchased from Fluka. Other reagents and solvents were analytical grade and used without further purification. The Schiff bases H_2L^1 was prepared according to the literature method.⁷ Elemental (C, H, and N) analyses were made on a Perkin-Elmer Model 240B automatic analyzer. IR spectra were recorded on an IR-408 Shimadzu 568 spectrophotometer. ¹H NMR spectra were recorded on a Bruker 300 MHz instrument.

2.2. Synthesis of H_2L^2

5-Fluorosalicylaldehyde (2.0 mmol, 0.28g) was dissolved in methanol (20 mL), to which was added dropwise a methanol solution (10 mL) of 2-hydroxy-1,3-propanediamine (1.0 mmol, 0.09 g) with stirring at room temperature. The mixture was stirred at room temperature for 30 min, and most of the solvent was removed by distillation. The yellow crystalline product was obtained by filtration.

- 66 Yield: 93%. IR data (cm⁻¹, KBr): 3370m, 1638s, 1587s, 1492s, 1450w, 1387w, 1318w,
- 67 1263s, 1216m, 1142m, 1090w, 1040m, 966w, 878m, 822s, 784s, 673w, 577w, 456w.
- ¹H NMR (300 MHz, DMSO) δ 12.72 (s, 2H, OH), 8.51 (s, 2H, CH=N), 7.35 (dd, J =
- 69 8.9, 3.1 Hz, 2H, ArH), 7.19 (td, J = 8.7, 3.2 Hz, 2H, ArH), 6.89 (dd, J = 9.0, 4.5 Hz,
- 70 2H, ArH), 4.04 (s, 1H, OH), 3.79 (dd, J = 12.1, 4.0 Hz, 2H, CH2), 3.61 (dd, J = 12.1,
- 71 6.6 Hz, 2H, CH₂). ¹³C NMR (75 MHz, DMSO) δ 156.98, 156.12, 153.02, 119.32,
- 72 119.01, 118.81, 116.71, 69.22, 62.87. Anal. Calcd. (%) for C₁₇H₁₆F₂N₂O₃: C, 61.1; H,
- 73 4.8; N, 8.4. Found (%): C, 61.3; H, 4.7; N, 8.3.

74 **2.3.** Synthesis of the molybdenum complex

- MoO₂(acac)₂ (0.1 mmol, 33.5 mg) in methanol (10 mL) was added with stirring to
- 76 H₂L (0.1 mmol, 31.8 mg) in methanol (10 mL). The mixture was stirred at refluxed
- for 30 min to give a yellow solution. The solution was left still at room temperature in
- air to give yellow block-shaped single crystals, which were collected by filtration and
- 79 dried in vacuum containing anhydrous CaCl₂. Yield: 52%. IR data (v, cm⁻¹): 1621 s,
- 80 1547 m, 1471 s, 1381 m, 1266 s, 1153 s, 1076 w, 977 m, 895 m, 820 m, 743 w, 703 w,
- 81 659 w, 620 w, 571 w, 515 w, 449 w, 415 w. UV-vis data in methanol [λ_{max} (nm), ε
- 82 $(L \cdot mol^{-1} \cdot cm^{-1})$]: 270, 12380; 325, 9310; 420, 2115. Anal. Calcd. (%) for
- 83 C₁₇H₁₄F₂MoN₂O₄: C, 46.0; H, 3.2; N, 6.3. Found (%): C, 45.7; H, 3.3; N, 6.2.

84 **2.4. Synthesis of the nickel complex**

- H_2L^2 (0.3 mmol, 100.2 mg) was dissolved in methanol (20 mL), to which was
- added a methanol-water solution (20 mL, V:V = 10:1) of nickel acetate tetrahydrate
- 87 (0.5 mmol, 124.5 mg) with stirring. The mixture was stirred at room temperature for
- 88 30 min to give a green solution, which was kept still to slow evaporate of the solvents.
- 89 Green block-like single crystals suitable for X-ray diffraction were formed. Yield:
- 90 37%. IR data (v, cm⁻¹): 3426 w, 1634 s, 1563 s, 1472 s, 1425 m, 1398 m, 1302 m,
- 91 1252 w, 1213 w, 1147 m, 1059 w, 957 w, 862 w, 817 s, 679 w, 616 w, 574 w, 475 w.
- 92 UV-vis data in methanol [λ_{max} (nm), ε (L·mol⁻¹·cm⁻¹)]: 361, 41900; 255, 48010; 235,
- 93 49132. Anal. Calcd. (%) for C₄₂H₄₂F₄N₄Ni₃O₁₅: C, 46.1; H, 3.9; N, 5.1. Found (%): C,
- 94 45.9; H, 4.0; N, 5.3.

95

2.5. X-ray diffraction

- Data were collected from selected crystals mounted on a glass fiber. The data for
- 97 the complexes were processed with SAINT⁸ and corrected for absorption using
- 98 SADABS. 9 Multi-scan absorption corrections were applied with ω scans. 10 The
- 99 structures of the complexes were solved by direct method using SHELXS-97 program

and refined by full-matrix least-squares techniques on F^2 using anisotropic displacement parameters. All non-hydrogen atoms were refined anisotropically. The water H atoms in the nickel complex were located in a difference Fourier map and refined isotropically, with O-H and H···H distances restrained to 0.85(1) and 1.37(2) Å, respectively. The remaining hydrogen atoms were placed at the calculated positions. The C8-C9-C10-O7 moiety in the nickel complex is disordered over two sites, with occupancies of 0.532(3) and 0.468(3). Crystallographic data for the complex are listed in Table 1. Selected bond lengths and angles are given in Table 2.

Table 1. Crystallographic data and structure refinement for the complexes

	The molybdenum complex	The nickel complex
Molecular formula	$C_{17}H_{14}F_2MoN_2O_4$	$C_{42}H_{42}F_4N_4Ni_3O_{15}$
Formula weight	444.24	1094.93
Crystal system	Monoclinic	Monoclinic
Space group	$P2_1/c$	$P2_1/n$
a, Å	10.689(2)	12.548(1)
b, Å	17.327(2)	13.188(1)
c, Å	9.001(1)	15.065(1)
eta, \circ	103.175(2)	112.789(3)
V, Å ³	1623.2(4)	2298.3(4)
Z	4	2
F(000)	888	1124
$\mu(MoK_{\alpha}), mm^{-1}$	0.857	1.305
Colleted reflections	14985	21744
Independent reflections	2885	4270
Observed reflections $(I \ge 2\sigma(I))$	2494	3077
Restraints/parameters	0/235	17/342
Goodness of fit on F^2	1.063	1.056
$R_{\rm int}$	0.0285	0.0439
R_1 , wR_2 $(I \ge 2\sigma(I)]^*$	0.0248, 0.0570	0.0588, 0.1660
R_1 , wR_2 (all data)*	0.0330, 0.0607	0.0876, 0.1914
$\Delta \rho_{\rm max}$, $\Delta \rho_{\rm min}$, $e \ {\rm \AA}^{-3}$	0.303, -0.354	1.028, -0.665

^{*} $R_1 = \sum ||F_0| - |F_c|| / \sum |F_0|, wR_2 = \left[\sum w(F_0^2 - F_c^2)^2 / \sum w(F_0^2)^2\right]^{1/2}.$

Table 2. Selected bond lengths (Å) and angles (°) for the complexes

Table 2. Selected bond religins (1) and angles () for the complexes								
The molybder	_							
Mo(1)-O(1)	1.9290(17)	Mo(1)–O(2)	2.0935(17)					
Mo(1)-O(3)	1.7016(17)	Mo(1)–O(4)	1.7040(18)					
Mo(1)-N(1)	2.317(2)	Mo(1)–N(2)	2.169(2)					
O(3)–Mo(1)–O(4)	104.27(9)	O(3)–Mo(1)–O(1)	102.08(8)					
O(4)–Mo(1)–O(1)	101.45(9)	O(3)–Mo(1)–O(2)	89.80(8)					
O(4)–Mo(1)–O(2)	159.93(8)	O(1)–Mo(1)–O(2)	89.22(7)					
O(3)–Mo(1)–N(2)	93.80(8)	O(4)–Mo(1)–N(2)	86.32(9)					
O(1)–Mo(1)–N(2)	159.85(8)	O(2)–Mo(1)–N(2)	78.42(7)					
O(3)–Mo(1)–N(1)	168.13(8)	O(4)–Mo(1)–N(1)	85.67(8)					
O(1)-Mo(1)-N(1)	81.88(7)	O(2)–Mo(1)–N(1)	79.00(7)					
N(2)–Mo(1)–N(1)	80.19(8)							
The nickel	complex							
Ni(1)-O(1)	2.061(3)	Ni(1)-O(2)	2.053(3)					
Ni(1)-O(6)	2.044(4)	Ni(2)–O(1)	1.995(3)					
Ni(2)–O(2)	1.990(3)	Ni(2)–O(3)	2.177(5)					
Ni(2)–O(5)	2.066(5)	Ni(2)–N(1)	2.014(4)					
Ni(2)–N(2)	2.016(5)							
O(6)-Ni(1)-O(6A)	180	O(6)-Ni(1)-O(2)	89.0(2)					
O(6)-Ni(1)-O(2A)	91.0(2)	O(2)-Ni(1)-O(2A)	180					
O(6)-Ni(1)-O(1)	90.1(1)	O(6)-Ni(1)-O(1A)	89.9(1)					
O(2)–Ni(1)–O(1)	79.4(1)	O(2)–Ni(1)–O(1A)	100.6(1)					
O(1)-Ni(1)-O(1A)	180	O(2)–Ni(2)–O(1)	82.5(1)					
O(2)–Ni(2)–N(1)	172.8(2)	O(1)–Ni(2)–N(1)	90.8(2)					
O(2)–Ni(2)–N(2)	90.2(2)	O(1)-Ni(2)-N(2)	171.5(2)					
N(1)–Ni(2)–N(2)	96.2(2)	O(2)–Ni(2)–O(5)	91.3(2)					
O(1)–Ni(2)–O(5)	90.7(2)	N(1)–Ni(2)–O(5)	91.5(2)					
N(2)–Ni(2)–O(5)	93.8(2)	O(2)–Ni(2)–O(3)	92.6(2)					
O(1)–Ni(2)–O(3)	90.2(2)	N(1)-Ni(2)-O(3)	84.7(2)					
N(2)–Ni(2)–O(3)	85.8(2)	O(5)–Ni(2)–O(3)	176.2(2)					
		I						

2.6. Catalytic oxidation

The complexes (0.001 mol·L⁻¹) and phenyl methyl sulfide (0.100 mol·L⁻¹) were dissolved at room temperature in a mixture of CH₂Cl₂ and CH₃OH (6:4) together with 1,3,5-trimethoxybenzene (0.100 mol·L⁻¹) as internal standard. The resulting solution was cooled to 283 K and H₂O₂ (35% w/w) added dropwise (0.125 mol·L⁻¹). An aliquot of the reaction solution (2.0 mL) was quenched with 5.0 mL of a stock solution of Na₂SO₃ (0.100 mol·L⁻¹) and extracted with dichloromethane (three times 4 mL). From the collected organic phases the solvent was removed under reduced pressure to complete dryness and the residue redissolved in deuterated chloroform (0.60 mL) and analyzed by ¹H NMR to determine the yield with reference to the internal standard 1,3,5-trimethoxybenzene.

3. Results and Discussion

3.1. Chemistry

Reaction of the Schiff base H_2L^1 with $MoO_2(acac)_2$, and H_2L^2 with $Ni(CH_3COO)_2$, respectively, afforded the molybdenum and nickel complexes. The complexes are soluble in DMF, DMSO, methanol, ethanol and acetonitrile. We have attempted to grow diffraction quality crystals from various solvents, however, well-shaped single crystals suitable for X-ray diffraction can only be obtained from methanol solution.

3.2. Structure Description of the Molybdenum Complex

The molecular structure of the complex is shown in Fig. 1. The coordination geometry around the Mo atom in the complex is octahedrally distorted. The Schiff base ligand coordinates to the Mo atom through two phenolate O and two imino N atoms, forming three six-membered chelate rings with the Mo atom. The other two sites are coordinated by two oxo groups. Atoms O(1), N(1), N(2) and O(3) located at the equatorial plane show a high degree of planarity, with mean deviation from the plane of 0.002(3) Å. The Mo(1) atom deviates from the least-squares plane defined by the four equatorial donor atoms by 0.185(2) Å in the direction of the axial atom O(4). The angular distortion in the octahedral coordination comes from the bites O(2)-Mo(1)-O(4) [159.93(8)°] and O(1)-Mo(1)-N(2) [159.85(8)°]. The dihedral angle between the two benzene rings of the Schiff base ligand is 112.0(5)°. In the complex, the coordinate bond lengths are comparable to those observed in molybdenum complexes with Schiff base ligands. The Mo(1)-O(2) and Mo(1)-N(1) bonds are much longer than usual, which are caused by the *trans* effects of the Mo=O bonds. The Mo=O bonds are also longer than usual, which might be caused by the formation

of hydrogen bonds with adjacent groups (Table 3). In the crystal of the complex,

molecules are linked through intermolecular C-H···O hydrogen bonds (Table 3), to

form a three dimensional network (Fig. 2).

3.3. Structure Description of the Nickel Complex

- 153 The molecular structure of the complex is shown in Fig. 3. The asymmetric unit of the
- 154 compound contains a linear trinuclear nickel(II) complex molecule and a water
- molecule of crystallization. The molecule of the complex possesses crystallographic
- two-fold rotation axis symmetry, with the inversion center located at the site of Ni(1)
- atom. There are three bridges across the Ni···Ni atom pairs, involving two phenolate O
- atoms of a Schiff base ligand, and an O–C–O moiety of a μ_2 - η^1 : η^1 -OAc group. The
- acetate bridges linking the central and terminal nickel atoms are mutually *trans*. The
- trinuclear nickel complex molecule consists of two NiL units connected to each other
- by a completely encapsulated third metal atom, Ni(1). The adjacent Ni(1)···Ni(2)
- 162 distance is 3.018(1) Å.

- The cage of Ni(1) is formed by phenolate bridges, O(1) and O(2), from the Schiff
- base ligands, and by two O atoms from two μ_2 - η^1 : η^1 -OAc ligands that furthermore
- 165 connect the central metal with the two outer metal atoms resulting in an octahedral
- environment. The coordination around Ni(1) atom displays only slight distortion. The
- bond distances Ni–O are relatively similar and range from 2.044(4) to 2.061(3) Å.
- The greatest deviation of the bond angles from those expected for an ideal octahedral
- 169 geometry is found for O(1)-Ni(1)-O(2) with 79.4(1)°, and O(1)-Ni(1)-O(2A) with
- 170 100.6(1)°. The remaining bond angles are close to the ideal values for the octahedral
- 171 coordination.
- The coordination around the inversion-related terminal Ni atoms is also octahedral,
- with two imino N and two phenolate O atoms from a Schiff base ligand defining the
- equatorial plane, and with two O atoms respectively from a μ_1 - η^1 : η^0 -OAc and a
- μ_2 - η^1 : η^1 -OAc ligands occupying the axial positions. The coordination around the
- terminal metal atoms also displays slight distortion. The greatest deviation of the bond
- angles from those expected for an ideal octahedral geometry is O(1)-Ni(2)-O(2)
- 178 (82.5(1)°), which is caused by the strain created by the four-membered chelate ring
- 179 Ni(1)–O(1)–Ni(2)–O(2).
- The NiL units in the complex are butterfly-shaped, with the dihedral angles formed
- by the two benzene rings of the Schiff base ligands of 57.5(5)°. In the crystal structure
- of the complex (Fig. 4), the methanol molecules are linked to the nickel complex

molecules through O–H···O hydrogen bonds (Table 3). In addition, there are $\pi \cdots \pi$ stacking interactions among the benzene rings defined by atoms C(1)/C(2)/C(3)/C(4)/C(5)/C(6) and C(12A)/C(13A)/C(14A)/C(15A)/C(16A)/C(17A) [symmetry code for A: -x, 1-y, 1-z; centroid-centroid distance 4.873(3) Å, the angle between the planes 57°; the perpendicular distance between the planes 3.593(6) Å] in the complex.

Table 3. Distances (Å) and angles (°) involving hydrogen bonding of the complexes

D–H···A	d(<i>D</i> –H)	d(H··A)	$d(D\cdots A)$	Angle(D–H···A)			
The molybdenum complex							
$C(3)$ - $H(3)$ ··· $O(3)^{i}$	0.93	2.57(3)	3.1980(6)	125(4)			
C(10)–H(10A)···O(4)	0.97	2.53(3)	2.8760(5)	101(5)			
C(11)–H(11)····O(3) ⁱⁱ	0.93	2.48(4)	3.1287(6)	127(5)			
C(13)–H(13)···O(4) ⁱⁱ	0.93	2.56(4)	3.2410(6)	131(5)			
The nickel complex							
O(7)–H(7A)···O(8) ⁱⁱⁱ	0.82	2.07(3)	2.77(2)	143(4)			

191 Symmetry codes: i: 1 - x, -y, -z; ii: 2 - x, -y, 1 - z.

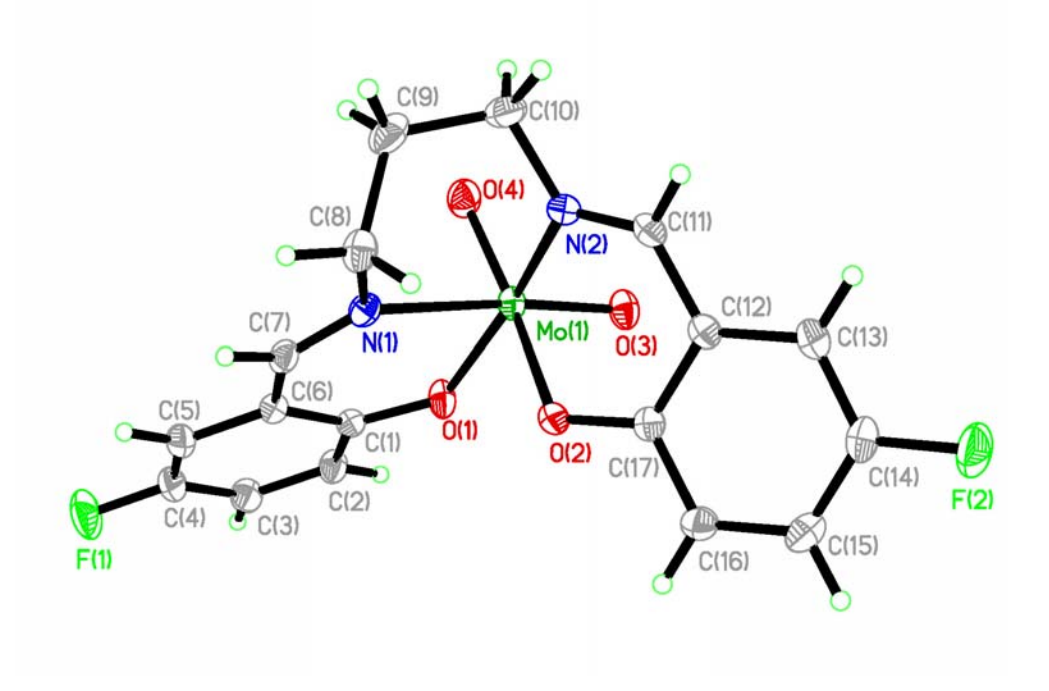


Fig. 1. Molecular structure of the molybdenum complex at 30% probability thermal ellipsoids.

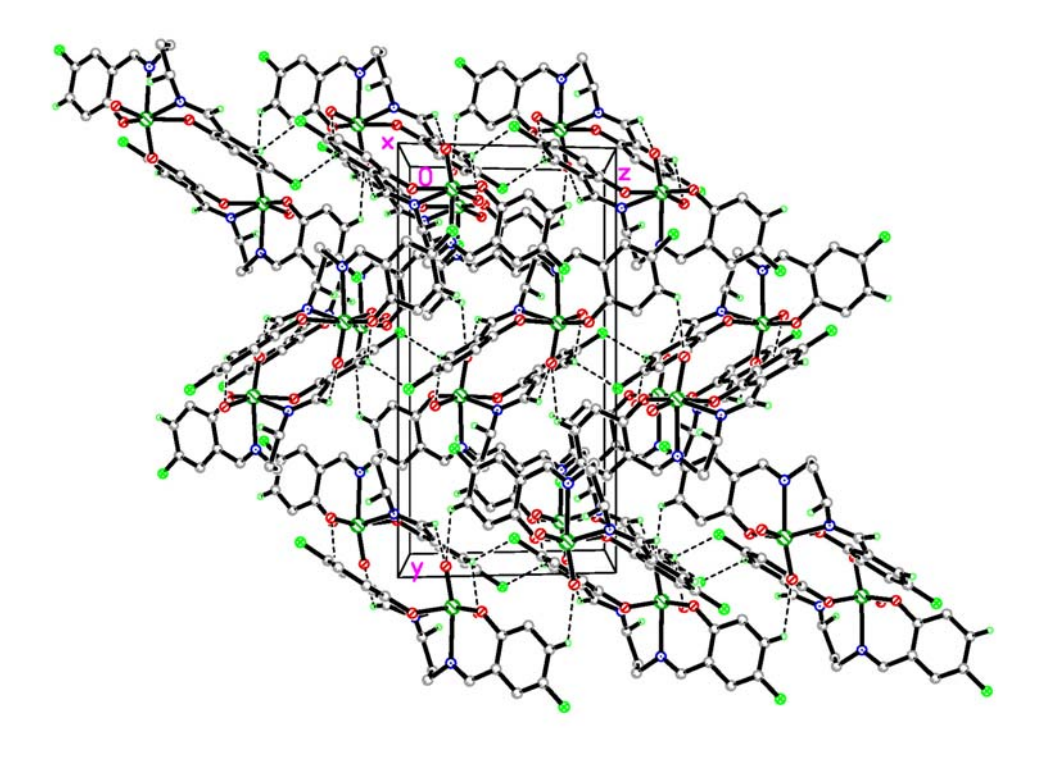


Fig. 2. Molecular packing structure of the molybdenum complex, viewed along the x-axis direction. Hydrogen bonds are drawn as dotted lines.

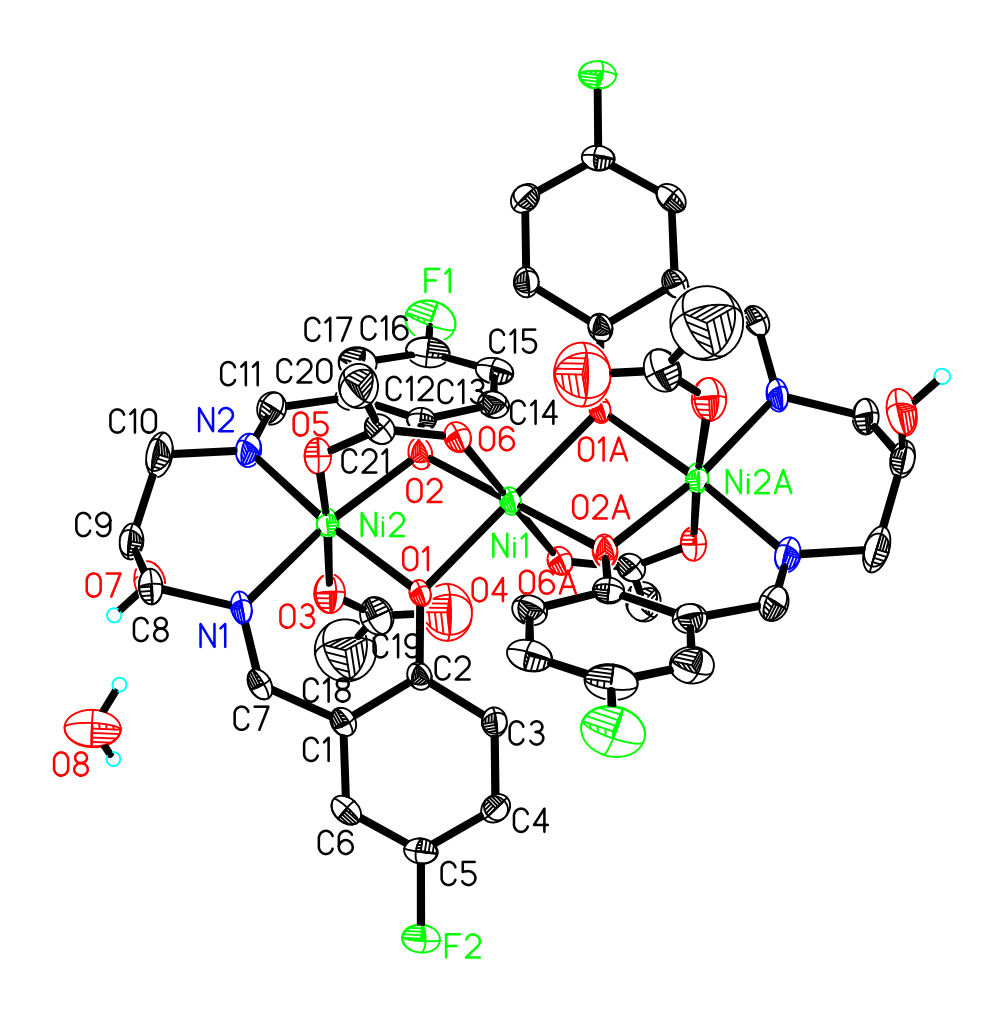


Fig. 3. Molecular structure of the nickel complex. Displacement ellipsoids are drawn at the 30% probability level and H atoms are shown as small spheres of arbitrary radii. Atoms labeled with the suffix A or unlabeled are related to the symmetry position -x, 1-y, 1-z.

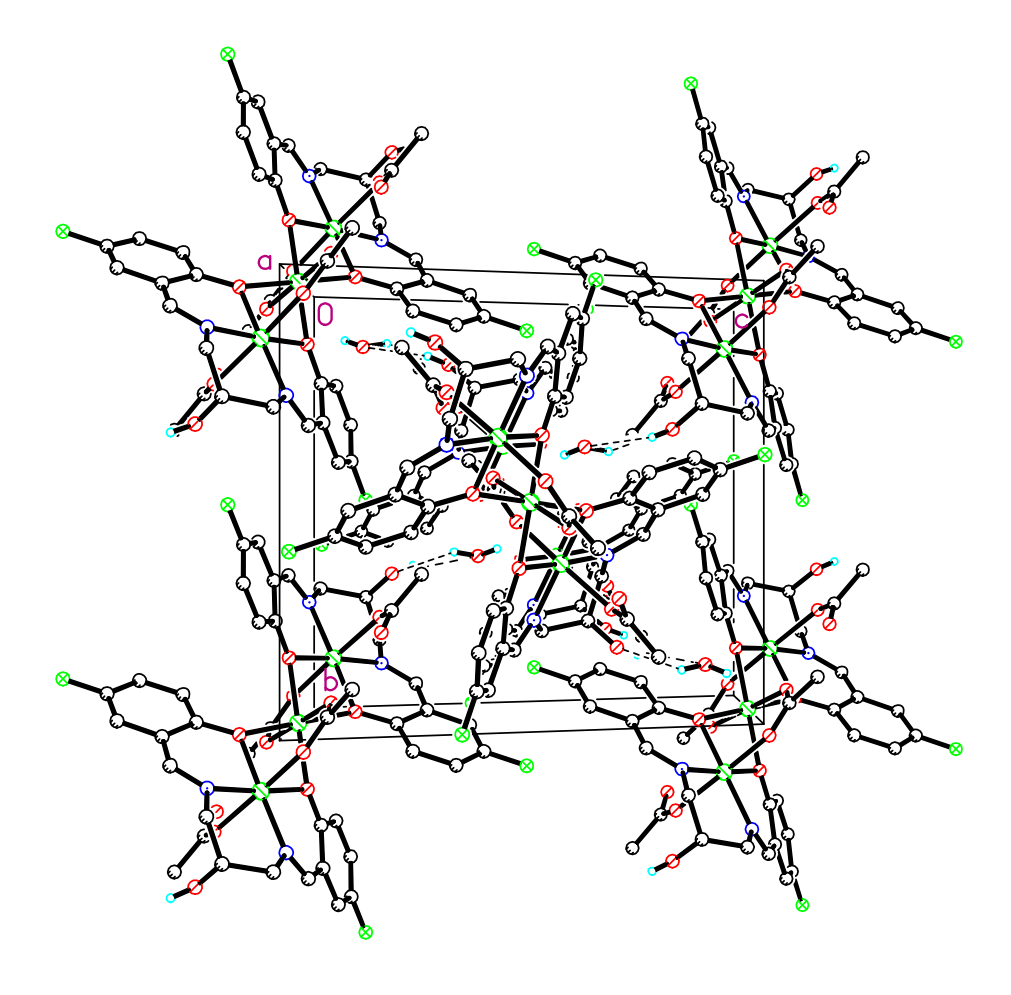


Fig. 4. Molecular packing diagram of the nickel complex, viewed along the a axis. Hydrogen bonds are drawn as dashed lines.

3.4. IR and UV-Vis Spectra

In the infrared spectra of the free Schiff bases, there showed stretching band attributed to C=N and OH at 1638-1645 and 3370 cm⁻¹, respectively. In the spectra of the complexes, the $v_{C=N}$ bands were observed at lower frequencies, viz. 1621-1634 cm⁻¹. In the spectrum of the molybdenum complex, there showed two prominent bands at 977 and 895 cm⁻¹, which attributed to dioxomolybdenum groups. In the spectrum of the nickel complex, there exhibits typical acetate vibrations $v_{asym}(OAc)$ at 1563 cm⁻¹ and $v_{sym}(OAc)$ at 1450 cm⁻¹. The bands due to $v_{C=O}$ are absent in both the free Schiff bases and the complexes. This suggests the formation of the azomethine groups, CH=N, during the condensation reaction of the starting material. The weak bands in

the low wave numbers are assigned to the Mo–O and Mo–N vibrations.

The electronic spectra of the complexes were recorded in methanol. In the molybdenum complex, there showed bands at 325 nm and weak band at 420 nm. The weak band is attributed to intra-molecular charge transfer transitions from the p_{π} orbital on the nitrogen and oxygen to the empty d orbitals of the metal. The intense band observed at 270 nm is assigned to intra-ligand π - π * transitions. In the nickel complex, the azomethine chromophore π - π * transition is located at 361 nm. The broad non-symmetric band with absorption maximum at 420 nm can be assigned as LMCT.

3.5. Catalytic Property of the Complexes

Catalytic oxidation test of the complexes on the oxidation of sulfides under homogeneous conditions in solution using methyl phenyl sulfide (thioanisol) as substrate is shown as Scheme 3. As oxidant hydrogen peroxide was used in a slight excess of 1.25 equivalents based on the sulfide substrate. Reactions were run with 1 mol% of catalyst based on the substrate at a temperature of 10 °C. NMR technique has been used to monitor the formation of the sulfoxides with 1,3,5-trimethoxybenzene (TMB) as internal standard to determine the yields. The reaction was started by the addition of hydrogen peroxide. A control reaction under the same condition without any complex present leads to less than 1% sulfide conversion within 4 h. In the presence of the molybdenum complex conversion of 94% of sulfide to the corresponding sulfoxide within 60 min reaction time was observed. After about 2 h in all cases the conversions of total amount of sulfide were completed. Under the given conditions no over oxidation to the sulfone could be detected. However, the nickel complex has no activity on the reaction. Thus, the molybdenum complex showed excellent catalytic property for the sulfoxidation reaction.

$$\begin{array}{c|c} S & & \\ \hline \\ H_2O_2/TMB \end{array}$$

Scheme 3. The sulfoxidation process.

246247

248

249

244

245

219

220

221

222

223

224

225

226

227

228

229

230

231

232

233

234

235

236

237

238

239

240

241

242

243

4. Supplementary materials

CCDC –1870626 and 1465136 contain the supplementary crystallographic data for this paper. The data can be obtained free of charge at

- 250 http://www.ccdc.cam.ac.uk/const/retrieving.html or from the Cambridge
- 251 Crystallographic Data Centre (CCDC), 12 Union Road, Cambridge CB2 1EZ, UK;
- 252 fax: +44(0)1223-336033 or e-mail: deposit@ccdc.cam.ac.uk.

254 **5. Acknowledgements**

255 This research was supported by the Top-class foundation of Pingdingshan

256 University (no. PXY-BSQD-2018006 and PXY-PYJJ-2018002).

257

258 **6. References**

- 1. (a) C. A. Gamelas, A. C. Gomes, S. M. Bruno, F. A. A. Paz, A. A. Valente, M.
- 260 Pillinger, C. C. Romao, I. S. Goncalves, *Dalton Trans.* **2012**, *41*, 3474-3484; (b) L.
- 261 S. Feng, J. S. Maass, R. L. Luck, *Inorg. Chim. Acta* **2011**, 373, 85-92; (c) M.
- Bagherzadeh, M. Amini, A. Ellern, L. K. Woo, *Inorg. Chem. Commun.* 2012, 15,
- 52-55; (d) S. Rayati, N. Rafiee, A. Wojtczak, *Inorg. Chim. Acta* **2012**, *386*, 27-35.
- 264 2. (a) B.I. Ceylan, Y. D. Kurt, B. Ulkuseven, *J. Coord. Chem.* **2009**, *62*, 757-766; (b)
- 265 M. N. Sokolov, M. A. Mikhailov, P. A. Abramov, V. P. Fedin, J. Struct. Chem.
- 2012, 53, 197-201; (c) S.-P. Gao, J. Coord. Chem. 2011, 64, 2869-2877.
- 267 3. (a) S. Mandal, R. Saha, B. Mahanti, M. Fleck, D. Bandyopadhyay, *Inorg. Chim.*
- Acta 2012, 387, 1-7; (b) M. A. Vazquez-Fernandez, M. I. Fernandez-Garcia, A. M.
- Gonzalez-Noya, M. Maneiro, M. R. Bermejo, M. J. Rodriguez-Douton,
- 270 *Polyhedron* **2012**, *31*, 379-385; (c) F. Habib, P.-H. Lin, J. Long, I. Korobkov, W.
- Wernsdorfer, M. Murugesu, *J. Am. Chem. Soc.* **2011**, *133*, 8830-8833.
- 4. (a) N. K. Ngan, K. M. Lo, C. S. R. Wong, *Polyhedron* **2012**, *33*, 235-251; (b) S.
- Duman, I. Kizilcikli, A. Koca, M. Akkurt, B. Ulkuseven, *Polyhedron* **2010**, *29*,
- 274 2924-2932; (c) R. D. Chakravarthy, K. Suresh, V. Ramkumar, D. K. Chand, *Inorg*.
- 275 Chim. Acta 2011, 376, 57-63; (d) C. P. Rao, A. Sreedhara, P. V. Rao, M. B.
- Verghese, K. Rissanen, E. Kolehmainen, N. K. Lokanath, M. A. Sridhar, I. S.
- 277 Prasad, J. Chem. Soc. Dalton Trans. 1998, 2383-2393.
- 278 5. (a) M. Mancka, W. Plass, *Inorg. Chem. Commun.* **2007**, 10, 677-680; (b) S. N.
- 279 Rao, N. Kathale, N. N. Rao, K. N. Munshi, *Inorg. Chim. Acta* 2007, 360,
- 280 4010-4016; (c) R. Dinda, S. Ghosh, L. R. Falvello, M. Tomas, T. C. W. Mak,
- 281 *Polyhedron* **2006**, *25*, 2375-2382.
- 282 6. (a) L. Wang, Y. J. Han, Q. B. Li, L. W. Xue, Russ. J. Coord. Chem. 2017, 43,
- 283 389-395; (b) Q.-B. Li, Y.-J. Han, G.-Q. Zhao, L.-W. Xue, *Acta Chim. Slov.* **2017**,

- 284 *64*, 500-505.
- 285 7. (a) L. Shi, Z.-P. Xiao, Z. Zhuang, H.-L. Zhu, Acta Crystallogr. 2007, E63, o4726;
- 286 (b) L.-W. Xue, Y.-J. Han, G.-Q. Zhao, Y.-X. Feng, J. Chem. Crystallogr. 2011, 41,
- 287 1599-1603.
- 8. Bruker, SMART and SAINT. Area Detector Control and Integration Software;
- Bruker Analytical X-ray Instruments Inc.: Madison, WI, USA, 1997.
- 9. G. M. Sheldrick, SADABS. Program for Empirical Absorption Correction of Area
- 291 Detector Data; University of Göttingen: Göttingen, Germany, 1997.
- 292 10. A. C. T. North, D. C. Phillips, F. S. Mathews, Acta Crystallogr. 1968, A24,
- 293 351-355.
- 294 11. G. M. Sheldrick, SHELXL-97. Program for the Refinement of Crystal Structures;
- 295 University of Göttingen: Göttingen, Germany, 1997.
- 12. (a) S. N. Rao, K. N. Munshi, N. N. Rao, M. M. Bhadbhade, E. Suresh, *Polyhedron*
- 297 **1999**, 18, 2491-2497; (b) W.-X. Xu, W.-H. Li, Synth. React. Inorg. Met.-Org.
- 298 Nano-Met. Chem. **2012**, 42, 160-164.
- 299 13. G. Romanowski, M. Wera, *Polyhedron* **2010**, *29*, 2747-2754.
- 300 14. T. Głowiak, L. Jerzykiewicz, J. A. Sobczak, J. J. Ziolkowski, *Inorg. Chim. Acta*
- **2003**, *356*, 387-392.
- 302 15. B.-H. Ye, X.-Y. Li, I. D. Williams, X.-M. Chen, *Inorg. Chem.* **2002**, 41,
- 303 6426-6431.